CHEMISTRY
A EUROPEAN JOURNAL

DOI: 10.1002/chem.200903457

Studies on Electronic Effects in O-, N- and S-Chelated Ruthenium Olefin-Metathesis Catalysts

Eyal Tzur,[a] Anna Szadkowska,[d] Amos Ben-Asuly,[a, b] Anna Makal,[e] Israel Goldberg,[c] Krzysztof Woźniak,[e] Karol Grela,*[d, e] and N. Gabriel Lemcoff*[a]

Abstract: A short overview on the structural design of the Hoveyda–Grubbs-type ruthenium initiators chelated through oxygen, nitrogen or sulfur atoms is presented. Our aim was to compare and contrast O-, N- and S-chelated ruthenium complexes to better understand the impact of electron-withdrawing and -donating substituents on the geometry and activity of the ruthenium complexes and to gain further insight into the *trans–cis* isomerisation process of the S-chelated complexes. To evaluate the different effects of chelating heteroatoms and to probe electronic effects on sulfur- and nitrogen-chelated latent catalysts, we synthesised a series of novel complexes. These catalysts were compared against two well-known oxygen-chelated initiators and a sulfoxide-chelated complex. The structures of the new complexes have been determined by single-crystal X-ray diffraction and analysed to search for correlations between the structural features and activity. The replacement of the oxygen-chelating atom by a sulfur or nitrogen atom resulted in catalysts that were inert at room temperature for typical ring-closing metathesis (RCM) and cross-metathesis reactions and showed catalytic activity only at higher temperatures. Furthermore, one nitrogen-chelated initiator demonstrated thermo-switchable behaviour in RCM reactions, similar to its sulfur-chelated counterparts.

Keywords: carbenes · chelates · ligand design · metathesis · ruthenium

Introduction

The great efficacy and scope of olefin metathesis reactions have induced much effort in the study of ruthenium carbene initiators. The successful achievements in this area have led to impressive catalysts that assist olefin metathesis with unprecedented efficiency.[1] Without a doubt, two of the most significant modifications on the original first-generation Grubbs ruthenium catalyst[2] were the substitution of one of the tricyclohexylphosphine ligands by a more potent sigma-electron donor, the N-heterocyclic carbene (second-generation Grubbs catalyst)[3] and the replacement of the second phosphine ligand by an *ortho*-isopropoxy benzylidene moiety capable of chelation (Hoveyda–Grubbs).[4] Predictably, alteration of the chelated benzylidene radically altered the reactivity of the catalysts. Changes in steric strain,[5] chelate ring size,[6] the chelated heteroatom[5–7] and electron density on the aromatic ring of the chelated benzylidenes[8] have been shown to afford catalysts with activities that range from latent[9] (no activity at room temperature), such as complex $\mathbf{1}_{cis}$ (Scheme 1), to one of the most reactive ruthenium catalysts to date. For example, Hoveyda–Grubbs

[a] E. Tzur, Dr. A. Ben-Asuly, Dr. N. G. Lemcoff
Department of Chemistry, Ben-Gurion University of the Negev
Beer-Sheva 84105 (Israel)
Fax: (+972) 86461740
E-mail: lemcoff@bgu.ac.il

[b] Dr. A. Ben-Asuly
Achva Academic College, Shikmim 79800 (Israel)

[c] Prof. I. Goldberg
Department of Chemistry, Tel-Aviv University
Tel Aviv 69978 (Israel)

[d] A. Szadkowska, Prof. K. Grela
Institute of Organic Chemistry PAS, Kasprzaka 44/52
01-224 Warszawa (Poland)
Fax: (+48) 22-343-2109
E-mail: klgrela@gmail.com

[e] A. Makal, Prof. K. Woźniak, Prof. K. Grela
Department of Chemistry, Warsaw University, Pasteura 1
02-093 Warzsawa (Poland)

Supporting information for this article is available on the WWW under http://dx.doi.org/10.1002/chem.200903457.

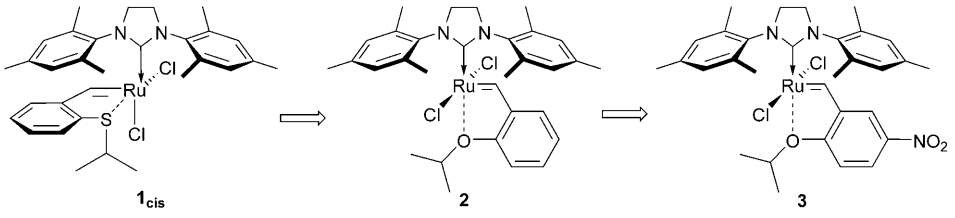

Scheme 1. Selected complexes exhibit different reactivity in metathesis reactions.

catalyst **2** has been successfully fine-tuned to increase its activity by the introduction of an electron-withdrawing group (EWG) to diminish the donor properties of the oxygen atom. As a result, nitro-substituted Hoveyda–Grubbs catalyst **3** has found a number of applications in various studies.

When mainly steric effects were probed, two different approaches were discerned. Firstly, the introduction of a bulky group *ortho* to the chelated heteroatom, such as in the Blechert system **5**,[10] and secondly, the direct substitution of the heteroatom with a bulkier group (complexes **4** and **6** in Scheme 2).[5] The most typical results demonstrated that the use of bulkier ligands promoted faster reactions.[4a,5a,11] Nonetheless, we find in the literature some examples that are not in accordance with this trend. For instance, Grubbs' imine-chelated initiator **6** promoted faster reaction with an isopropyl derivative than with a *tert*-butyl derivative (Scheme 2).[5b]

When electronic effects were probed, the results were even more puzzling at first glance. The activation of ruthenium-chelated catalysts by EWGs is well established; most prominently, as detailed above, we find that in complex **3** the introduction of a nitro group *para* to the chelated isopropoxy unit significantly enhanced reaction initiation.[8a] On the other hand, Grela and Kim showed that the introduction of two methoxy groups, prominent electron-donating groups (EDGs), had a comparable (albeit less pronounced) activation effect.[8b] A similar observation in chiral Ru-based complexes was also made, by the group of Hoveyda.[8f] In addition, a study by Blechert et al.[8c] shows that when moderate EWGs such as fluoro (**7** and **8**) or trifluoromethyl (**9**) are introduced *para* to the benzylidene carbon atom or the chelated oxygen atom (Scheme 3) the rate of ring-closing metathesis (RCM) of diallyl tosylamide remains relatively unchanged. In other words, the position of the EWG did not alter the catalyst reactivity noticeably, however, the position of the isopropoxy EDG greatly influenced the reaction rate (complexes **10** and **12** in Scheme 3). Moreover, a methyl group *para* to the chelated isopropoxy moiety, as in **11**, had a significantly stronger retardation effect than the stronger electron-donating alkoxy group in **12** (Scheme 3). Blechert et al. concluded that

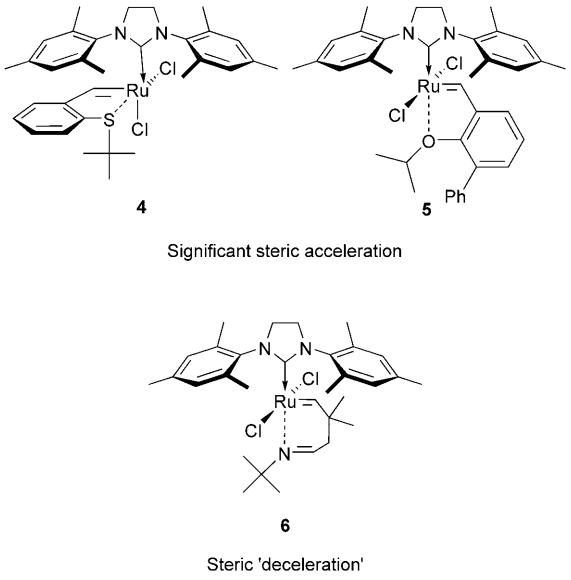

Scheme 2. Steric effects in chelated alkylidene catalysts.

to be able to predict catalyst initiation rates mainly the electronic effects on the benzylidene carbon must be taken into account. Recently, the lack of linear relationships between

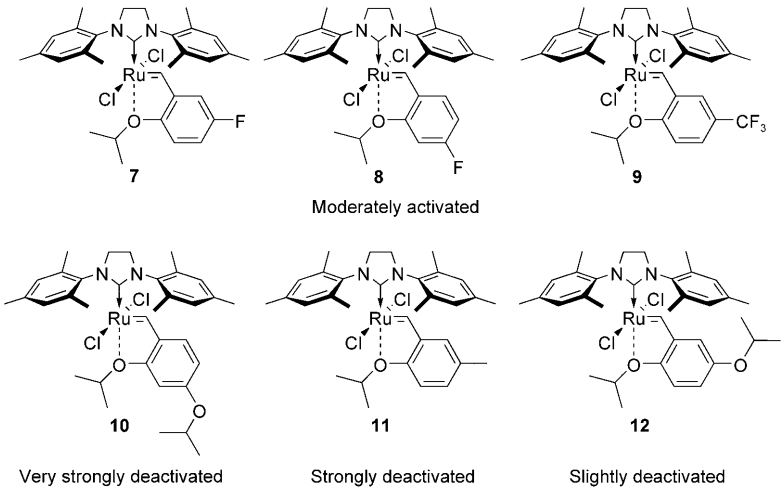

Scheme 3. Electronic effects on Blechert initiators.

electronic and steric effects for ruthenium Hoveyda–Grubbs-type catalysts was discussed in yet another example of modification of these catalysts by electronic effects.[8e]

The design of efficient catalytic switches necessitates a comprehensive understanding of the chemical changes that can be made to a catalyst to deactivate it: the off position. Some examples of switchable metathesis catalysts in the literature include catalysts that may be activated/deactivated by changes in the acidity of the media,[12] by changes in temperature,[7a] by the addition/removal of deactivating ligands[13] or by photo-activation.[14] For example, Lemcoff et al. recently disclosed a series of sulfur-chelated latent catalysts that were able to promote olefin metathesis reactions only at elevated temperatures and showed thermo-switchable behaviour for RCM.[5a,7a,c]

To evaluate the effect of the chelated heteroatom and to probe electronic effects in sulfur- and nitrogen-chelated latent catalysts, we synthesised novel complexes **27–31**. These were compared with well-known initiators **2** and **3**, which are chelated through an oxygen atom, and with the recently published sulfoxide-chelated complex **13**.[11]

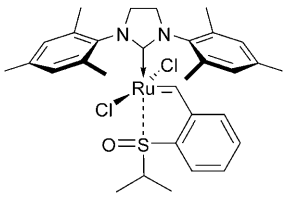

13

The new complexes were characterised with the aid of single-crystal X-ray structures, and their catalytic performance was evaluated in RCM and cross-metathesis (CM) reactions at room temperature and above.

Results and Discussion

Synthesis of ruthenium complexes: The styrene derivatives **19–23** were synthesised as shown in Scheme 4.

The commercially available aldehyde starting materials were treated with potassium carbonate and the corresponding nucleophile in dry DMF to afford the substitution products **14–18** (Scheme 4). Subsequent treatment with methyltriphenylphosphonium salt and potassium *tert*-butoxide gave the desired styrenes **19–23**.

An S(O)-chelated ligand that contained an EWG ($-NO_2$) was prepared in accordance with the procedure shown in Scheme 5. Aldehyde **17** was transformed into the sulfoxide-substituted styrene **25** by bromine-promoted oxidation followed by a Wittig reaction.

Sulfone styrene **26** was synthesised by straightforward peroxide oxidation of **23** (Scheme 6).

The final step in the synthesis of novel complexes **27–31** involved typical ligand-exchange reactions of complex **32**

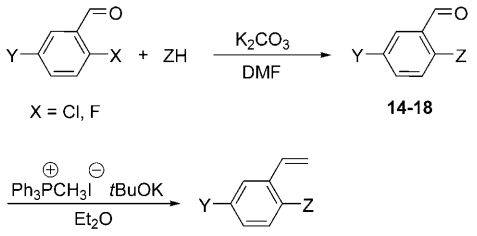

X = Cl, F

14-18

19-23

aldehyde	styrene	Y	Z-
14	**19**	H	
15	**20**	NO_2	
16	**21**	OCH_3	
17	**22**	NO_2	
18	**23**	H	—SH

Scheme 4. Synthesis of ligands **19–23**.

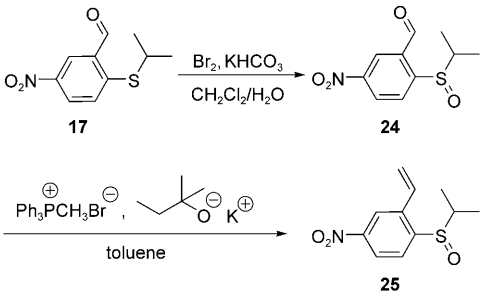

17 **24** **25**

Scheme 5. Synthesis of styrene **25**.

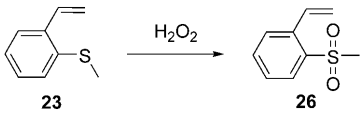

23 **26**

Scheme 6. Synthesis of sulfone styrene **26**.

with styrenes **19–22** and **25**, respectively, in the presence of CuCl in dichloromethane (Scheme 7). All our attempts to obtain a sulfone-chelated complex with styrene **26** were unsuccessful, which implied that the oxygen atoms in the sulfone are probably not good chelating atoms in these complexes.

Structural characterisation of the prepared complexes: Complexes **27–31** were fully characterised by NMR spectroscopy and FAB-MS (see the Supporting Information). Single crystals of good quality for X-ray analysis were also obtained for all new complexes (Figure 1). Several structures of N- and O-chelated ruthenium have already been deposited in Cambridge Structural Database[15] and these were included in calculations of the average bond lengths and angles (Figure 2). The list of reference codes for the utilised struc-

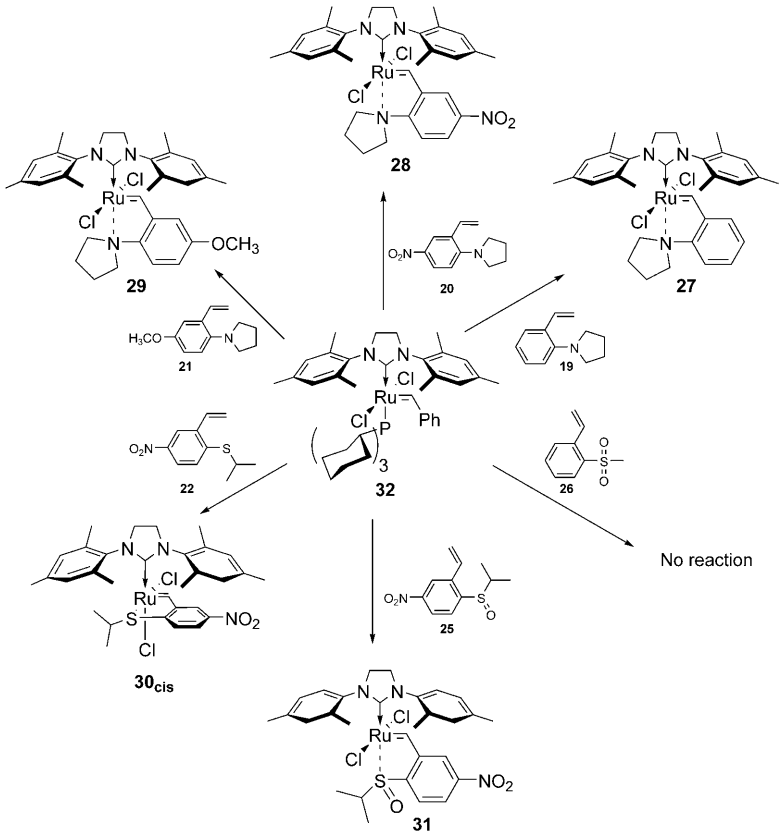

Scheme 7. Synthesis of N- and S-chelated complexes **27**–**31** by ligand exchange.

tures is enclosed in the Supporting Information (Part III, Table A1).

Structural comparison of the O-, S- and N-substituted Hoveyda-type catalysts: The following similarities and differences in X-chelated ruthenium complexes (X=O, N, S(O), S) were found. Firstly, the Ru–X distance increases with increasing atomic number, although it is significantly shorter in sulfoxide complexes than in sulfide complexes. Also the X–C29 bond length increases monotonically from N to O to S (Figure 2a), whereas the C23–C28 bond length tends to decrease. The C1–Ru and the X–C28 bond lengths are shortest for the O-chelates due to the sp^2 hybridisation of the oxygen atom and charge flows. Interestingly, the N- and S-chelates show similar C1–Ru lengths, which may also reflect the fact that in both cases the X atom is sp^3 hybridised. Additionally, the Ru–Cl average bond length tends to be shorter for O- and S(O)-chelates. The C22–C23 bond length is the most conserved across all the chelates (Figure 2a).

The angle variability is greater for the valence angles, especially those which involve the X atom. In particular the C28-X-C29 angle values for the N- and O-chelates differ significantly from the values obtained when X=S or S(O). The Cl-Ru-Cl angle varies within a small range of 157.5–160°. The C1-Ru-X angle tends to be smaller for the nitrogen and

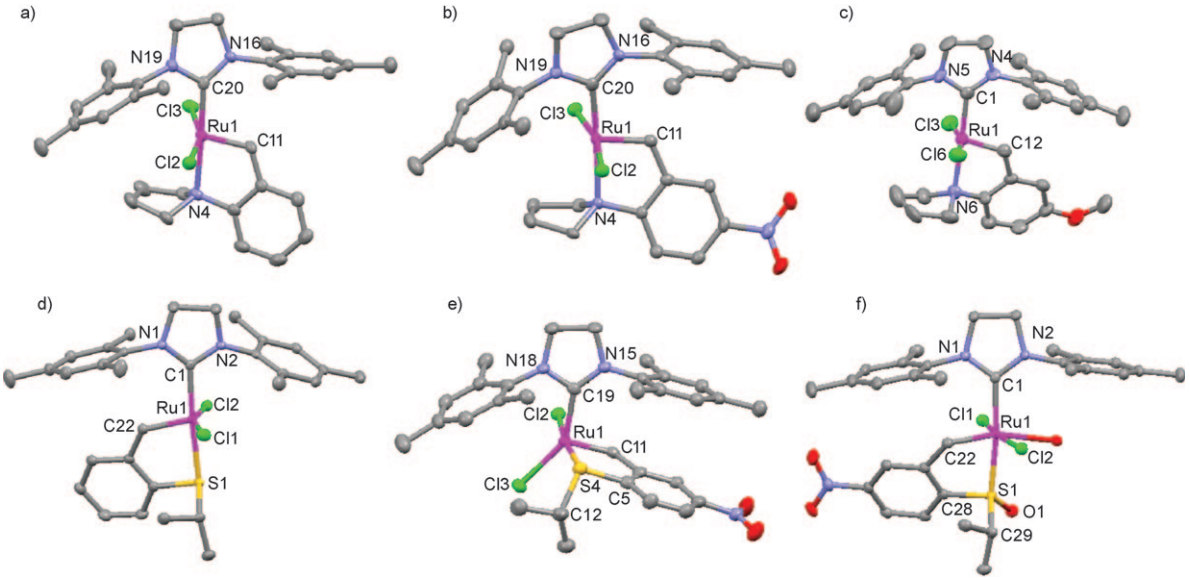

Figure 1. Crystal structure of a) **27**, b) **28**, c) **29**, d) $\mathbf{1}_{trans}$, e) $\mathbf{30}_{cis}$, f) **31**. Ellipsoids are drawn at 50% probability. Hydrogen atoms are omitted for clarity.

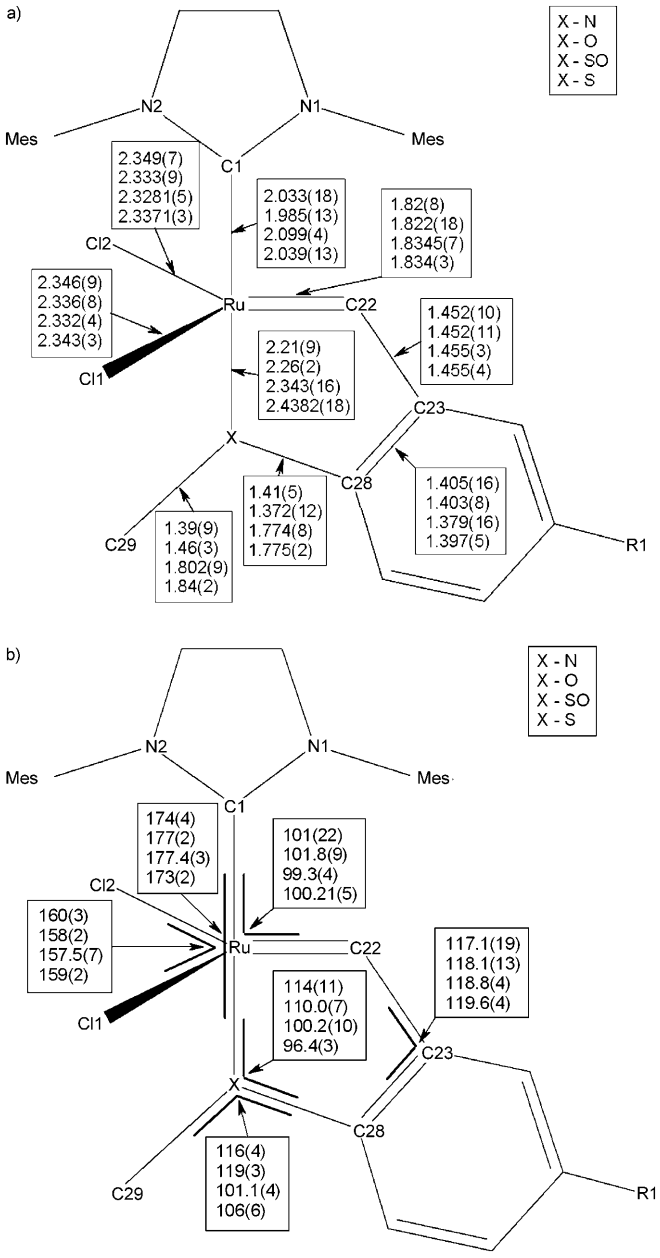

Figure 2. Selected a) average bond lengths [Å] and b) average valence angles [°] for different Ru–X coordinated complexes (averages of the complexes in this article and others; see Table A1 in the Supporting Information). The values refer to the chelated heteroatom (X) in the following order: X = N, O, S(O), S.

sulfur atoms (173.2 and 174.4°, respectively) and larger for the O- and S(O)-chelates (177°). However, only the differences observed for angles and bond lengths that involve the X atom are significantly larger than the standard deviation of the parameters in question.

Sulfur and oxygen atom hybridisation: The valence angles around the chelated oxygen atom adopt values close to 110 and 120° and are, on average, 10° higher than the analogous angles around the sulfur atom (Figure 2b). The sum of the three valence angles around the oxygen atom deviate from 360° by no more than 3° (see Part III of the Supporting Information, Table A1), which clearly indicates a planar configuration and, therefore, sp^2 hybridisation at the oxygen atom. The valence angles around the chelated sulfur atom tend to be much smaller and the bond angle values (Figure 2b) suggest partial sp^3d hybridisation of sulfur. This can be explained by the second-order Jahn–Teller effect, that is, by the presence of a very low-lying excited state of the sulfur atom, in which the 3d orbitals are occupied. Mixing with the ground state lowers the ground-state energy and results in the geometry modifications. For instance, the Ru1-S-C28 angle in $\mathbf{30}_{cis}$ is smaller than 100° and the C28-S-C29 angle is 100°, rather than the 109.5° ideally expected in the case of sp^3 hybridisation. The Ru1-X-C29 angle is more than 120°. The corresponding angles for $\mathbf{1}_{trans}$ (Figure 1 in Part III of the Supporting Information) have values of 96, 102 and 114°, respectively, and in the case of sulfoxides the angles Ru1-S-C28 and C28-S-C29 have values around 100°.

Impact of EWG or EDG substituents on the geometry of complexes: The overall impact of EWG or EDG substitution on the structure of the main chelate is quite small. Most of the differences between the samples are well below three standard deviations for a given parameter, in particular the N–Ru distance appears invariable. Similarly, the N3–C29, N3–C30, C22–C23 and C23–C24 bond lengths may be considered insensitive to the substitutions. There are small changes in the bond lengths in the substituted benzene ring, which may be described as the increased differentiation of the bonds lengths (decreased aromaticity, measured by the harmonic oscillator measure of aromaticity (HOMA)[19] index). Bond C24–C25 is shortened, whereas bonds C25–C26 and C27–C28 get longer. Still, the changes are on the border of statistical significance (Table 1). The only parameters that seem to change significantly upon nitro substitution are the Ru–Cl1 bond length (elongated by 0.02 Å) and the Cl1-Ru1-Cl2 angle, which is broadened by over 7°. The plane of the benzylidene ligand is also more rotated with respect to the plane that contains ruthenium, C1 and N3. The torsion angle of C22-Ru1-N3-C28 increases by 4° upon substitution, which illustrates this rotation. *p*-Methoxy substitution, in the case of **29**, results in a general decrease in length of most bonds in the benzene moiety, as well as significant reduction of the C22=Ru and Cl2–Ru bond lengths. On the other hand, the Cl1–Ru bond length gets longer. The angles in the benzene moiety behave in correlation with elongation

Table 1. Mean bond lengths, standard deviations and calculated HOMA index from experimental geometries of the compounds **27**, **28** and **29**.

Complex	Mean bond length of aromatic C–C bonds[Å]	Bond standard deviation [Å]	HOMA
27	1.391	0.008	0.99
28	1.391	0.010	0.98
29	1.380	0.016	0.93

or reduction of the adjacent bond lengths. There is also an interesting increase (2°) in the value of the C1-Ru-N3 angle. The Cl-Ru-Cl angle adopts a value of 164°, which is 4° larger than in the unsubstituted structure and 3° smaller than in the nitro-substituted catalyst. The relative rotation of the benzylidene moiety with respect to the plane containing Ru_1, C_1 and N_3 is illustrated by the C22-Ru1-N3-C28 torsion angle, which increases upon methoxy substitution.

There are some significant differences in the relative orientation of the mesityl (Mes) substituents with respect to the main complex site. In the case of **27**, the plane of the imidazole ring is bent away from the Cl2 chlorine atom with respect to the C1–Ru1 bond. The Mes arms do not locate above the benzylidene unit in the main complex and are bent towards each other and the Cl1 chlorine atom. In the case of structure **28**, the C1–Ru1 bond is coplanar with imidazole. One of the Mes arms locates directly above the benzylidene moiety in the main complex and the main axes of the two Mes groups are parallel. In the case of the methoxy substitution in the structure **29**, the imidazole plane and Ru–C1 bond are again collinear, but the Mes substituents are bent, similar to **28**. However, these effects may result from different crystal packing of the structures as well as from substitution effects. Comparisons of the bond lengths and angles in the structures of **27**, **28** and **29** are displayed in Figure 3.

Relative reactivity studies: To explore the reactivity profiles of the catalysts, various olefin substrates were reacted. Tables 2–4 summarise the results for RCM and CM reactions. Overall, and in line with many of our studies, the trend observed for RCM of diethyl diallylmalonate (Figure 4) was observed in the other metathesis reactions as well.

Catalysts containing O-donor ligands: The phosphine-free systems **2** and **5**, introduced by the groups of Hoveyda[4a] and Blechert,[4b,9] display high reactivity levels towards electron-deficient substrates, such as acrylonitrile and fluorinated olefins. Excellent air stability, easy storage and handling, the possibility of catalyst reuse and of catalyst immobilisation make clear the advantages of this system. In spite of the promising application profile observed in reactions of **2**, this catalyst proved to initiate more slowly than other phosphine systems, probably as the result of electronic factors (*i*PrO→Ru electron donation).[15] More detailed studies on catalytic activation resulted in the preparation of nitro-substituted Hoveyda catalyst **3**.[8a,b] The strong EWG *para* to the isopropoxy donor in **3** weakens the *i*PrO→Ru chelation and facilitates initiation of the catalytic cycle. Consequently, **3** possesses dramatically enhanced catalyst performance in model RCM and CM reactions (Table 2).

Oxygen-chelated initiators **2** and **3** exhibited good activity in model metathesis reactions (Table 2, entries 1–4). However, nitro-substituted complex **3** serves as an effective RCM catalyst for the formation of disubstituted double bonds even at 0 °C. Furthermore, the potential of a nitro-substitut-

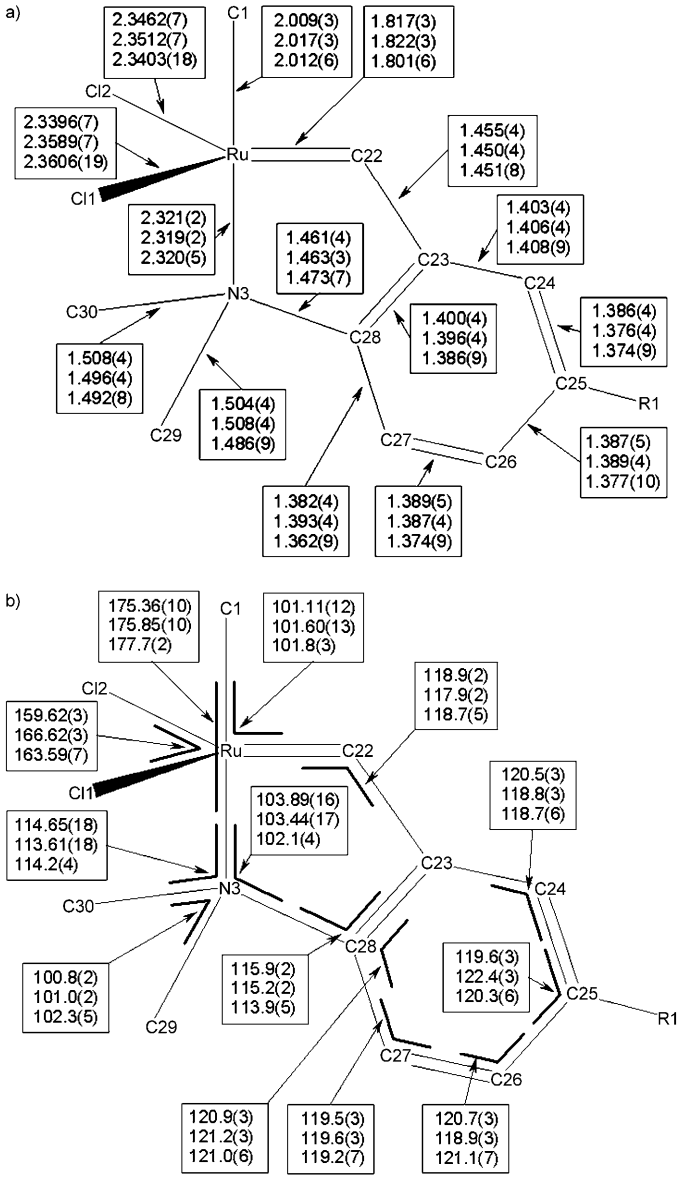

Figure 3. Selected a) bond lengths [Å] and b) valence angles [°] in the structures of **27**, **28** and **29**. The values are reported in the following order: R1 = H (**27**), R1 = NO_2 (**28**), R1 = OMe (**29**).

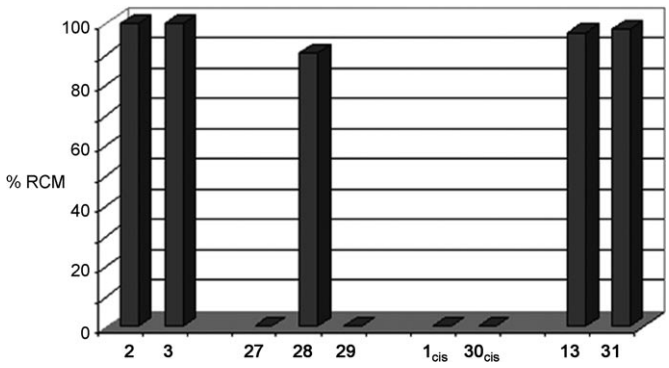

Figure 4. RCM conversions [%] of diethyl diallylmalonate (0.1 M) with several catalysts (1 mol%) in toluene after 24 h at 24 °C.

Table 2. Formation of disubstituted double bonds promoted by catalysts **2** and **3**.[a]

Entry	Substrate	Product	Catalyst [mol%]	Yield [%]	T [°C]	t [h]
1	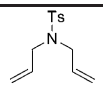		**2** (1)	40	0	4
			3 (1)	92	0	2
2	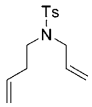		**2** (1)	48	0	4
			3 (1)	99	0	1
3	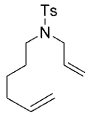		**2** (1)	50	0	4
			3 (1)	99	0	1
4	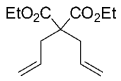		**2** (2.5)	52	0	8
			3 (2.5)	78	0	8
5	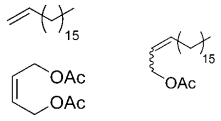		**2** (1)	37	24	6
			3 (1)	89	24	6

[a] Conditions: 1–2.5 mol% of catalyst, [substrate] = 0.02 M, dichloromethane, yields determined by GC.

ed catalyst for more challenging metathesis reactions has been proved in a CM reaction (Table 2, entry 5).

Catalysts containing N-donor ligands: The results of typical RCM and CM reactions of the new N-chelated complexes **27, 28** and **29** are summarised in Table 3.

N-Chelated complex **27** was inert to typical RCM reactions at room temperature and showed activity only at higher temperatures (Table 3, entry 4). However, nitro-substituted N-chelated catalyst **28** showed an impressive acceleration effect. Thus, the introduction of an EWG ($-NO_2$) transformed a room-temperature latent catalyst into an active catalyst (Figure 4 and Table 3). To determine the effects of EDGs in latent catalysts, we explored the activity of catalyst **29**. As expected, catalyst **29** showed no activity at room temperature and was less active than **27** at higher temperatures (Table 3, entries 1, 3 and 5). However, the diethyl diallylmalonate RCM rate was higher than that observed for catalyst **27** at these temperatures (Table 3, entry 4), similar to the results obtained by Hoveyda et al. with the chiral O-chelated complexes.[8f] The benchmark RCM reaction of diethyl diallylmalonate with catalysts **27** and **29** was followed by GC–MS and the results are presented in Figure 5.

*Thermo-switchable behaviour of catalyst **27***: Additionally, we examined the thermo-switchable behaviour of **27**. Reactions with intermittent periods of heating and cooling (55 °C/25 °C) were carried out in toluene under a nitrogen atmosphere. As shown in Figure 6, catalyst **27** demonstrated a thermo-switchable behaviour, similar to our previous observations on sulfur-chelated ruthenium benzylidene catalysts.[7a]

Table 3. Formation of disubstituted double bonds promoted by catalysts **27**, **28** and **29**.[a]

Entry	Substrate	Product	Catalyst	Yield [%]	T [°C]	t [h]
1			**27**	18	55	2
			27	89	55	24
			28	37	24	2
			28	90	24	24
			29	8	55	2
			29	61	55	24
2	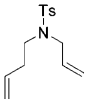		**27**	95	55	21
			28	99	24	7
			29	98	55	24
3	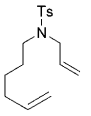		**27**	55[b]	55	92
			28	25[b]	24	2
			29	28[b]	55	48
4	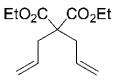	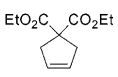	**27**[c]	0	24	16
			27	45	55	6
			27	78	55	24
			27[d]	82	55	69
			28	93	24	27
			28[e]	100	24	0.5
			29	0	24	24
			29	70	55	6
			29	86	55	24
5	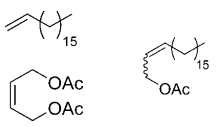		**27**	56	55	5
			27	78	55	24
			28	63	24	5
			28	85	24	24
			29	35	55	5
			29	52	55	24

[a] Conditions: 1 mol% catalyst, [substrate] = 0.1 M in toluene, yields determined by GC. [b] Olefin isomerisation affords an additional seven-membered ring product, longer reaction times promoted higher yields of the isomerisation product. [c] [substrate] = 0.2 M. [d] 0.1 mol% catalyst. [e] In dichloromethane.

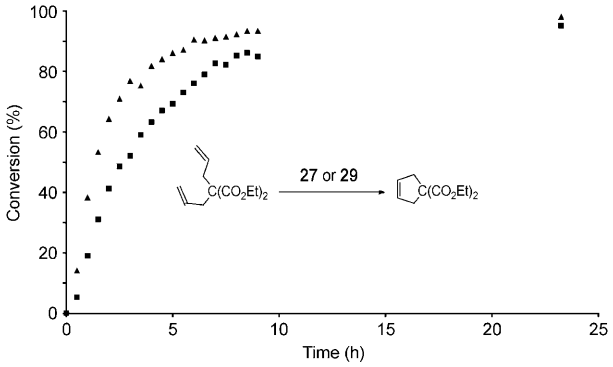

Figure 5. Catalytic behaviour of **27** (■) and **29** (▲) in the RCM of diethyl diallylmalonate (c = 0.1 M, toluene, T = 65 °C, 1 mol% catalyst). Products analysed by GC–MS.

Catalysts containing S-donor ligands: Noting the significant activation effect of the nitro group in catalyst **28** (as well as in **3**), we tested the effect of the addition of a nitro group to latent S-chelated complex $\mathbf{1}_{cis}$. Surprisingly, nitro-substituted complex $\mathbf{30}_{cis}$ was found to be inert to RCM reactions at

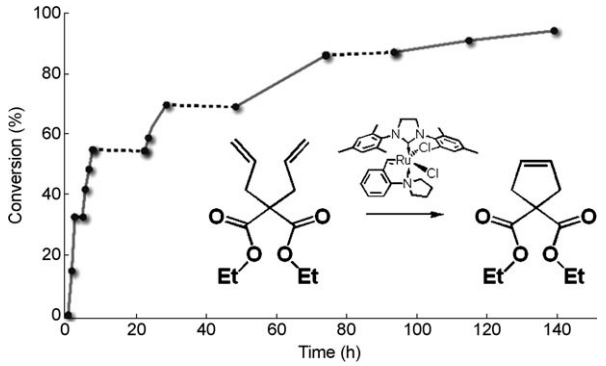

Figure 6. Thermo-switchable behaviour of catalyst **27** in the RCM of diethyl diallylmalonate ($c=0.1$ M, toluene, 1 mol% catalyst). Dashed line: 24°C; solid line: 55°C.

room temperature and showed activity only at higher temperatures (Table 4, entry 4, and Figure 4). Due to the negligible activation obtained by this procedure, we decided to compare the catalytic activity of S-chelated initiators $\mathbf{1}_{cis}$ and $\mathbf{30}_{cis}$ with their sulfoxide counterparts **13** and **31**. Sulfoxide initiator **31** turned out to be the most active from the group of S-chelated catalysts. However, tests of catalytic activity showed that catalyst **31** proceeded in typical RCM reactions just slightly faster than initiator **13**. The most significant differences in catalyst performance between complexes **13** and **31** were observed for more demanding substrates (RCM of eight-membered rings and CM; Table 4, entries 3 and 5). Initiators $\mathbf{1}_{cis}$ and $\mathbf{30}_{cis}$ required high temperatures to induce metathesis reactions (90°C). Based on the performance in model reactions, shown in Table 4, we conclude that electronic effects seem to play a decisive role in increasing the catalytic activity of the sulfoxide-chelated complexes, whereas sulfide-chelated complexes remain latent.

To determine the kinetic profiles of the active sulfoxide catalysts **13** and **31** and to test a more challenging substrate for RCM, we measured the progress of the RCM reaction of diethyl allylmethallylmalonate (Figure 7). Both catalysts showed high activity with this substrate and almost full conversion was achieved in under 2 h at 40°C with 1 mol% catalyst in toluene.

Table 4. Formation of disubstituted double bonds promoted by catalysts $\mathbf{1}_{cis}$, **13**, $\mathbf{30}_{cis}$ and **31**.

Entry	Substrate	Product	Catalyst	Yield [%]	T [°C]	t [h]
1			**1**	75	90	28
			30	86	90	28
			13	70	24	24
			31	85	24	24
2	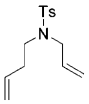		**1**	94	90	18
			30	98	90	18
			13	86	24	24
			31	93	24	24
3	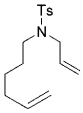		**1**	31[b]	90	48
			30	32[b]	90	48
			13	42	24	24
			31	87	24	24
4	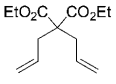	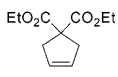	**1**	0	24	24
			1	84	90	48
			1[c]	55	90	48
			30	0.2	24	24
			30	91	90	41
			13	97	24	24
			31	98	24	24
5	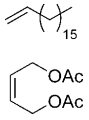		**1**	64	90	47
			30	57	90	42
			13	19	24	24
			31	53	24	24

[a] Conditions: [substrate] = 0.1 M in toluene, yields determined by GC. [b] Olefin isomerisation gives an additional seven-membered ring product. [c] 0.1 mol% catalyst.

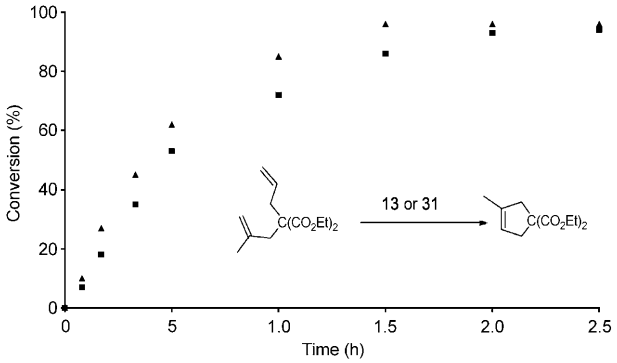

Figure 7. Catalytic behaviour of catalysts **13** (■) and **31** (▲) in the RCM of diethyl allylmethallylmalonate ($c=0.1$ M, toluene, $T=40$°C, 1 mol% catalyst). Products analysed by GC.

Kinetic isomerisation of $\mathbf{1}_{trans}$ to $\mathbf{1}_{cis}$: The relative stability of both isomers (*trans* and *cis*) provided the opportunity to measure the kinetics of the isomerisation process by integration of the characteristic benzylidene protons in the ^{1}H NMR spectrum of **1**. Deuterated dichloromethane, CD_2Cl_2, was chosen for measuring kinetic isomerisation of compound **1**. This process is shown in Figure 8. The results of this experiment showed that complex $\mathbf{1}_{trans}$ converts completely into $\mathbf{1}_{cis}$ after 50 h at 23°C. As shown in Figure 8, the data was fitted by an exponential relationship with correlation coefficient $R^2=0.9974$ and a calculated rate constant $k=1.2\times10^{-2}$ h^{-1}.

***Trans–cis* isomerisation**: It appears that the O-, N- and S(O)-chelates are more stable in the *trans* conformation, while S-chelates isomerise to the *cis* isomer.[17a] From a structural point of view, this could be attributed to the preferred sp^{3}d hybridisation of the sulfur atom and the steric effects that result from it. The structure of $\mathbf{30}_{cis}$ (Figure 1e) illustrates that if the sulfur atom displayed sp^2 hybridisation (and therefore a planar configuration of the linked substituents) then the isopropyl ligand in the *cis* conformation could have been in steric conflict with one of the Mes substituents. Notably, there are few examples of crystallographic structures of Ru–O and Ru–N chelates that display *cis*-dichloro

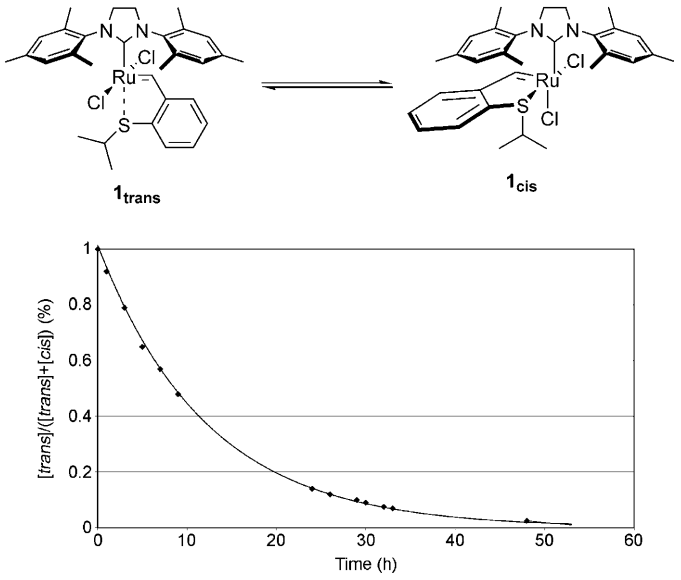

Figure 8. Kinetic isomerisation (^{1}H NMR spectroscopy) of $\mathbf{1}_{trans}$ to $\mathbf{1}_{cis}$ in CD_2Cl_2 at 23 °C.

coordination.[7b,17] In these cases, the chelated heteroatom is enclosed within a six-membered aromatic ring, well-ordered in the case of an aliphatic nitrogen atom and disordered in the case of an oxygen atom. In $\mathbf{1}_{cis}$ and $\mathbf{30}_{cis}$, the structure of the ligands does not entail steric clashes with the Mes moiety in the *cis* coordination. It is possible that the unoccupied 3d orbitals of the sulfur atom play a crucial part in the formation of transition states in the isomerisation process. The fact that the *cis* isomer was not observed for the sulfoxide-chelated catalysts would support such a hypothesis because, in the case of sulfoxides, the sulfur atom hybridisation is closer to sp^3. Therefore, the d orbitals have a smaller impact on the sulfur bonding and, moreover, the presence of the oxygen atom could shield possible interactions of the sulfur d orbitals with the Ru or Cl orbitals.

Conclusion

We have put forward a series of new ruthenium bidentate benzylidene catalysts based on sulfur and nitrogen chelation. These novel catalysts were thoroughly characterised and studied by spectroscopic and crystallographic techniques, which showed that EWG and EDG substituents have a minor effect on the structures of the catalysts. Our study also shows that latent nitrogen-chelated ruthenium benzylidenes may be strongly activated by reducing the electron density on the chelating aromatic group. In contrast, the introduction of EWGs on the sulfur-chelated benzylidene complexes could not awaken the latent catalysts. In this case, only direct oxidation of the sulfide ligand to a chiral (racemic) sulfoxide activated the dormant catalyst. This oxidation also transformed the geometry from a relatively inert *cis*-dichloro form to a more common *trans*-dichloro configuration. The introduction of a nitro group in the sulfoxide-chelated complex enhanced its reactivity, especially in demanding cases (RCM of eight-membered rings and CM). The study of latent metathesis catalysts and the means to activate them has important practical applications and it may also provide vital insights into the intricate mechanism of the metathesis reactions of strongly chelated complexes.

Experimental Section

General: All reagents were of reagent grade quality, purchased commercially from Sigma, Aldrich or Fluka and used without further purification. All solvents were dried and distilled prior to use. Purification by column chromatography was performed on Davisil Chromatographic silica gel (40–60 μm). TLC analyses were performed by using Merck precoated silica gel (0.2 mm) aluminium-backed sheets. Gas chromatography data was obtained under standard conditions with an Agilent 6850 GC equipped with an Agilent 5973 MSD and an Agilent HP5-MS column. NMR spectra were recorded on Bruker DPX200, Avance III 400 or DPX500 instruments. Chemical shifts (δ, ppm) are reported relative to Me_4Si as the internal standard or relative to the residual solvent peak. MS data was obtained by using a Bruker Daltonics Ion-Trap MS Esquire 3000 Plus equipped with atmospheric pressure chemical ionisation (APCI).

General procedure for synthesis of aldehydes (14–18): The corresponding benzaldehyde (16.1 mmol), potassium carbonate (17.1 mmol) and the appropriate nucleophile (17.1 mmol) were dissolved in DMF (10 mL) in a 50 mL round-bottomed flask under dry nitrogen and topped with a reflux condenser. The reaction mixture was heated at 55–80 °C for 24 h. After cooling, the mixture was added to saturated aqueous potassium carbonate solution (50 mL) and extracted with diethyl ether or dichloromethane (3×50 mL). The extracts were dried over anhydrous magnesium sulfate and evaporated under reduced pressure. The crude product was purified by chromatography on silica gel to afford the desired aldehyde.

Compound ***14***: The yellow-brown oil was purified by chromatography on silica gel (95:5 petroleum ether (60–80)/dichloromethane) to afford **14** as a yellow oil (2.20 g, 78 %). ^{1}H NMR (200 MHz, $CDCl_3$): δ = 1.98 (m, 4H), 3.36 (m, 4H), 6.81 (m, 2H), 7.38 (dt, J = 1.9, 7.6 Hz, 2H), 7.70 (dd, J = 1.6, 7.8 Hz, 1H), 10.08 ppm (s, 1H); ^{13}C NMR (50 MHz, $CDCl_3$): δ = 25.9, 52.6, 114.5, 116.4, 122.9, 133.1, 135.9, 134.1 190.1 ppm; MS (EI): *m*/*z* (%): 39 (9), 51 (17), 65 (11), 77 (41), 91 (35), 106 (86), 118 (91), 130 (18), 146 (46), 156 (13), 175 (100).

Compound ***15***: The yellow-brown solid was purified by recrystallisation from hot ethanol to afford **15** as a yellow solid (2.30 g, 65 %). ^{1}H NMR (200 MHz, $CDCl_3$): δ = 2.06 (m, 4H), 3.44 (m, 4H), 6.77 (d, J = 9.7 Hz, 1H), 8.16 (dd, J = 2.8, 9.4 Hz, 1H), 8.58 (d, J = 2.8 Hz, 1H), 9.98 ppm (s, 1H); ^{13}C NMR (50 MHz, $CDCl_3$): δ = 25.8, 52.9, 114.3, 120.8, 128.6, 131.3, 136.7, 151.8 187.8 ppm; MS (EI): *m*/*z* (%): 41 (6), 51 (8), 63 (8), 70 (18), 77 (14), 91 (12), 105 (16), 117 (26), 131 (6), 145 (12), 151 (100), 164 (45), 173 (13), 190 (8), 220 (79).

Compound ***16***: The crude product was purified by chromatography on silica gel (5:1 petroleum ether (60–80)/ethyl acetate) to afford **16** as a yellow oil (0.80 g, 30 %). ^{1}H NMR (200 MHz, $CDCl_3$): δ = 1.98 (m, 4H), 3.34 (m, 4H), 3.79 (s, 3H), 6.86 (d, J = 3.1 Hz, 1H), 7.05 (dd, J = 3.1, 9.0 Hz, 1H), 7.27 (s, 1H), 10.21 ppm (s, 1H); ^{13}C NMR (50 MHz, $CDCl_3$): δ = 25.7, 53.6, 55.7, 112.2, 116.9, 123.3, 123.9, 146.7, 151.9, 190.3 ppm; MS (EI): *m*/*z* (%): 134 (37), 136 (50), 148 (17), 149 (27), 162 (21), 176 (11), 190 (54), 204 (27), 205 (100), 206 (13).

Compound ***17***: The yellow-brown solid was filtered, washed with water and purified by chromatography on silica gel (10:1 petroleum ether (60–80)/diethyl ether) to give **17** as a yellow solid (1.81 g, 50 %). ^{1}H NMR (200 MHz, $CDCl_3$): δ = 1.46 (d, J = 6.9 Hz, 6H), 3.67 (septet, J = 6.9 Hz, 1H), 7.55 (d, J = 8.7 Hz, 1H), 8.32 (dd, J = 2.5, 8.7 Hz, 1H), 8.66 (d, J = 2.5 Hz, 1H), 10.3 ppm (s, 1H); ^{13}C NMR (50 MHz, $CDCl_3$): δ = 22.5, 36.6, 127.2, 127.4, 127.9, 133.4, 144.7, 150.8, 189.1 ppm; MS (EI): *m*/*z* (%): 43

(67), 69 (28), 108 (30), 125 (13), 136 (53), 149 (45), 166 (33), 182 (100), 183 (92), 192 (11), 210 (22), 225 (69).

Compound ***18***:[5a] The crude product was purified by chromatography on silica gel (1:1 *n*-hexane/ dichloromethane) to give **18** as a yellow oil (2.08 g, 85%). ^{1}H NMR (200 MHz, $CDCl_3$): $\delta = 2.49$ (s, 3H), 7.24–7.58 (m, 3H), 7.80 (dd, $J = 1.4$, 7.6 Hz, 1H), 10.25 ppm (s, 1H).

Compound 24: A solution of **17** (0.338 g, 1.5 mmol) in dichloromethane (10 mL) and a solution of $KHCO_3$ (1.18 g) in H_2O (10 mL) were mixed vigorously. A solution of bromine (0.264 g, 1.93 mmol) in dichloromethane (1.5 mL) was added dropwise (each drop was added after partial decolourisation of the mixture). After 20 min a flat spatula of solid Na_2SO_3 and dichloromethane (40 mL) were added. The organic phase was separated, washed with brine and dried over anhydrous $MgSO_4$. The solvent was evaporated under reduced pressure and the residue was purified by column chromatography (3:1–1:1 *c*-hexane/ethyl acetate) to give **24** as yellow crystals (0.250 g, 1.04 mmol, 70%). M.p. 118-120°C; ^{1}H NMR (400 MHz, $CDCl_3$): $\delta = 0.93$–0.98 (d, $J = 7.1$ Hz, 3H), 1.58–1.63 (d, $J = 7.1$ Hz, 3H), 3.12 (septet, $J = 7.1$ Hz, 1H), 8.40–8.46 (m, 1H), 8.62–8.68 (m, 1H), 8.78–8.84 (m, 1H), 10.16 ppm (s, 1H); ^{13}C NMR (100 MHz, $CDCl_3$): $\delta = 12.0$, 18.6, 53.4, 128.1, 128.2, 133.6, 149.3, 154.2, 189.9 ppm; IR (KBr): $\tilde{\nu} = 3372$, 3080, 3061, 3018, 2977, 2930, 2867, 1956, 1854, 1736, 1693, 1603, 1574, 1528, 1464, 1413, 1382, 1367, 1351, 1314, 1231, 1199, 1170, 1142, 1129, 1107, 1057, 1037, 1023, 1013, 952, 926, 914, 875, 852, 821, 743, 722, 704, 670, 577, 562, 538, 517, 502, 451, 433 cm^{-1}; MS (EI): *m*/*z* (%): 39 (18), 41 (22), 43 (41), 75 (10), 136 (20), 152 (14), 181 (34), 82 (100), 183 (14), 199 (68), 200 (14); HRMS (EI): *m*/*z*: calcd for $C_{10}H_{11}O_4SN$: 241.04088 $[M]^+$; found: 241.04034; elemental analysis calcd (%) for $C_{10}H_{11}O_4SN$: C 49.78, H 4.60, S 13.29, N 5.81; found: C 49.63, H 4.58, S 13.14, N 5.78.

General procedure for synthesis of styrenes (19–23): Methyl triphenylphosphonium iodide (0.78 g, 1.94 mmol) was dissolved in diethyl ether (15 mL) in a 50 mL round-bottomed flask at 0°C under dry nitrogen. Potassium *tert*-butoxide (0.24 g, 2.08 mmol) was added in one portion and the mixture was stirred for 10 min at RT. Aldehyde (**14–18**) (1.39 mmol) was added in one portion at 0°C and the reaction mixture was stirred for 24 h at RT. The mixture was added to saturated aqueous sodium bicarbonate solution (100 mL) and was extracted with dichloromethane (3× 50 mL). The combined organic extracts were dried over anhydrous magnesium sulfate and evaporated under reduced pressure. The crude product was purified by chromatography on silica gel to afford the desired styrene.

Compound ***19***: The crude product was purified by chromatography on silica gel (95:5 petroleum ether (60–80)/dichloromethane) to give **19** as a bright yellow oil (0.15 g, 62%). ^{1}H NMR (200 MHz, $CDCl_3$): $\delta = 1.95$ (m, 4H), 3.23 (m, 4H), 5.22 (dd, $J = 1.8$, 10.9 Hz, 1H), 5.59 (dd, $J = 1.8$, 17.3 Hz, 1H), 6.92 (m, 2H), 7.01 (dd, $J = 10.9$, 17.3 Hz, 1H), 7.21 (dt, $J = 1.8$, 7.6 Hz, 1H), 7.42 ppm (dd, $J = 1.8$, 7.6 Hz, 1H); ^{13}C NMR (50 MHz, $CDCl_3$): $\delta = 24.9$, 51.8, 112.3, 115.5, 120.0, 127.9, 128.1, 129.4 136.6, 148.4 ppm; MS (EI): *m*/*z* (%): 39 (5), 51 (7), 65 (4), 77 (21), 103 (11), 117 (32), 130 (100), 144 (60), 173 (67).

Compound ***20***: The crude product was purified by chromatography on silica gel (2:1 petroleum ether (60–80)/diethyl ether) to give **20** as an orange-brown solid (0.16 g, 89%). ^{1}H NMR (200 MHz, $CDCl_3$): $\delta = 1.97$ (m, 4H), 3.50 (m, 4H), 5.28 (dd, $J = 1.2$, 10.9 Hz, 1H), 5.54 (dd, $J = 1.2$, 17.2 Hz, 1H), 6.61 (d, $J = 9.0$ Hz, 1H), 7.98 (dd, $J = 10.9$, 17.4 Hz, 1H), 7.99 (dd, $J = 2.8$, 9.3 Hz, 1H), 8.14 ppm (d, $J = 2.8$ Hz, 1H); ^{13}C NMR (50 MHz, $CDCl_3$): $\delta = 25.8$, 51.8, 112.3, 115.0, 124.5, 125.3 126.1, 136.5 138.0, 152.3 ppm; GC–MS (EI): *m*/*z* (%): 39 (5), 51 (6), 63 (7), 77 (13), 89 (10), 103 (15), 116 (18), 129 (24), 143 (27), 157 (13), 171 (51), 175 (86), 189 (50), 218 (100).

Compound ***21***: The yellow-brown oil was purified by chromatography on silica gel (1:0–4:1 petroleum ether (60–80)/diethyl ether) to give **21** as a yellow oil (0.57 g, 82%). ^{1}H NMR (200 MHz, $CDCl_3$): $\delta = 1.91$ (m, 4H), 3.07 (m, 4H), 3.80 (s, 3H), 5.23 (dd, $J = 1.6$, 10.8 Hz, 1H), 5.62 (dd, $J = 1.6$, 17.4 Hz, 1H), 6.77 (dd, $J = 3.0$, 8.7 Hz, 1H), 6.94 (d, $J = 8.7$ Hz, 1H), 7.02 (d, $J = 3.0$ Hz, 1H), 7.04 ppm (dd, $J = 10.8$, 17.4 Hz, 1H); ^{13}C NMR (50 MHz, $CDCl_3$): $\delta = 24.4$, 52.5, 55.5, 112.3, 113.1, 113.5, 117.7, 131.9, 135.3, 142.0, 154.5 ppm; MS : *m*/*z* (%): 39 (3), 51 (3), 65 (4), 77 (7), 91 (8), 117 (16), 132 (11), 160 (71), 174 (14), 188 (100), 203 (79).

Compound ***22***: The crude product was purified by chromatography on silica gel (4:1 petroleum ether (60–80)/diethyl ether) to give **22** as a yellow oil (0.50 g, 81%). ^{1}H NMR (200 MHz, $CDCl_3$): $\delta = 1.37$ (d, $J = 6.6$ Hz, 6H), 3.56 (septet, $J = 6.6$ Hz, 1H), 5.50 (dd, $J = 0.9$, 10.9 Hz, 1H), 5.80 (dd, $J = 0.9$, 17.2 Hz, 1H), 7.09 (dd, $J = 10.9$, 17.2 Hz, 1H), 7.40 (d, $J = 8.7$ Hz, 1H), 8.04 (dd, $J = 2.5$, 8.7 Hz, 1H), 8.30 ppm (d, $J = 2.5$ Hz, 1H); ^{13}C NMR (50 MHz, $CDCl_3$): $\delta = 22.8$, 37.1, 118.4, 120.9, 122.3, 128.2, 132.8, 138.4, 144.5, 145.5 ppm; GC–MS (EI): *m*/*z* (%): 39 (3), 63 (3), 69 (3), 89 (8), 133, (11), 134 (100), 135 (11), 163 (10), 180 (35), 223 (15).

Compound ***23***:[5a] The crude product was purified by chromatography on silica gel (petroleum ether (60–80)) to give **23** as a colourless oil (0.33 g, 79%). ^{1}H NMR (200 MHz, $CDCl_3$): $\delta = 2.43$ (s, 3H), 5.32 (dd, $J = 1.2$, 10.9 Hz, 1H), 5.67 (dd, $J = 1.2$, 17.4 Hz, 1H), 7.05–7.26 (m, 4H), 7.46 ppm (dd, $J = 10.9$, 17.4 Hz, 1H).

Compound 25: In a Schlenk flask, solid methyltriphenylphosphonium bromide (0.41 g, 1.15 mmol) and toluene (6 mL) were placed under argon. Potassium *tert*-pentylate (1.7 M in toluene, 0.67 mL, 1.15 mmol) was added dropwise at 5°C. The reaction mixture was warmed to RT and stirred for 2 h. The mixture was cooled to 5°C and a solution of **24** (0.23 g, 0.96 mmol) in toluene (4 mL) was added, the mixture was allowed to warm to RT and was stirred overnight. A saturated aqueous solution NH_4Cl (15 mL) was added, the aqueous layer was extracted with *tert*-butyl methyl ether (3×20 mL) and the organic layer was dried over anhydrous $MgSO_4$. The solvent was evaporated under reduced pressure and the product was purified by short-column chromatography (2:3 *c*-hexane/ethyl acetate) to give **25** as a yellow solid (0.168 g, 0.7 mmol, 73%). M.p. 69–71°C; ^{1}H NMR (500 MHz, $CDCl_3$): $\delta = 0.99$–1.02 (d, $J = 7.0$ Hz, 3H), 1.35–1.38 (d, $J = 7.0$ Hz, 3H), 2.91 (septet, $J = 6.9$ Hz, 1H), 5.59 (d, $J = 11$ Hz, 1H), 5.94 (d, $J = 17.2$ Hz, 1H), 6.89 (dd, $J = 11.0$, 17.2 Hz, 1H), 8.04–8.06 (m, 1H) 8.26–8.28 (m, 1H), 8.36–8.37 ppm (m, 1H); ^{13}C NMR (125 MHz, $CDCl_3$): $\delta = 12.6$, 17.4, 53.4, 120.8, 120.8, 126.6, 129.9, 137.0, 147.2 149.7 ppm; IR (KBr): $\tilde{\nu} = 3134$, 3093, 3082, 3064, 2969, 2930, 2871, 2090, 2062, 1941, 1879, 1865, 1813, 1736, 1690, 1628, 1598, 1568, 1523, 1454, 1415, 1384, 1366, 1346, 1313, 1294, 1242, 1179, 1168, 1129, 1094, 1068, 1031, 989, 982, 939, 931, 902, 914, 878, 846, 798, 750, 740, 694, 668, 653, 591, 567, 560, 534, 514, 501, 481, 471, 438, 408 cm^{-1}; MS (EI): *m*/*z* (%): 43 (18), 121 (7), 133 (7), 134 (82), 135(6), 163 (9), 180 (100), 181 (13), 197 (53), 239 (7); HRMS (EI): *m*/*z*: calcd for $C_{11}H_{13}O_3SN$: 239.06162 $[M]^+$; found: 239.06217; elemental analysis calcd (%) for $C_{10}H_{11}O_4SN$: C 55.21, H 5.48, S 13.40, N 5.85; found: C 55.33, H 5.48, S 13.33, N 5.74.

Compound 26:[18] Styrene **23** (69 mg, 0.46 mmol) was added to a solution of 30% aqueous H_2O_2 (0.8 mL), sodium dodecyl sulfate (6.4 mg, 0.022 mmol) and 37% aqueous HCl (4.5 μL) and the reaction mixture was stirred overnight at RT. The reaction mixture was added to a saturated aqueous solution of sodium sulfate (20 mL) and extracted with ethyl acetate (3×10 mL). The crude product was purified by chromatography on silica gel (2:1 petroleum ether/ethyl acetate), followed by a second column chromatography (9:1 petroleum ether/ethyl acetate) to give the pure sulfone **26** (5.9 mg, 0.032 mmol, 7%).

General procedure for catalyst preparation (27–30): Styrene (**14–18**) (0.14 mmol), cuprous chloride (0.17 mmol) and second-generation Grubbs catalyst (0.14 mmol) were dissolved in dichloromethane (6 mL) in a 10 mL round-bottomed flask topped with a reflux condenser under dry nitrogen. The reaction mixture was heated at reflux temperature for 3–5 h. The resulting mixture was concentrated to 2–3 mL CH_2Cl_2. The crude product was purified by chromatography on silica gel to afford the desired catalyst.

Compound ***27***: The crude product was purified by chromatography on silica gel (7:3 *n*-hexane/acetone) to give **27** as a green solid (75.0 mg, 84%). Crystals suitable for X-ray analysis were obtained by slow diffusion between hexanes and a solution of **22** in dichloromethane at −18°C. ^{1}H NMR (500 MHz, CD_2Cl_2, 260 K): $\delta = 1.18$ (m, 2H), 1.54 (m, 3H), 1.56 (s, 2H), 2.32 (s, 3H), 2.36 (s, 6H), 2.43 (s, 3H), 2.49 (m, 2H), 2.52 (s, 6H), 3.81 (m, 2H), 4.11 (s, 4H), 6.85 (d, $J = 7.3$ Hz, 1H), 7.00 (s, 2H), 7.07 (s, 2H), 7.19 (t, $J = 7.3$ Hz, 1H), 7.20 (d, $J = 8.1$ Hz, 1H), 7.58 (t, $J =$

7.3 Hz, 1H), 16.89 ppm (s, 1H); ^{13}C NMR (125 MHz, CD_2Cl_2, 240 K): δ = 17.8, 20.2, 20.5, 20.7, 22.1, 50.6, 51.5, 58.1, 119.9, 122.2, 127.9, 128.3, 129.0, 133.5, 137.1, 137.6, 138.3, 138.5, 139.6, 147.1, 155.3, 169.9, 209.7, 302.0 ppm; HRMS (FAB): *m*/*z*: calcd for $C_{32}H_{39}Cl_2N_3Ru$: 637.16 $[M]^+$; found: 637.13.

Compound ***28***: The crude product was purified by chromatography on silica gel (7:3 *n*-hexane/acetone) to give **28** as a dark-green solid (54.0 mg, 52%). Crystals suitable for X-ray analysis were obtained by slow diffusion between hexanes and a solution of **23** in dichloromethane at 4°C. ^{1}H NMR (500 MHz, CD_2Cl_2, 216 K): δ = 1.11 (m, 2H), 1.57 (m, 2H), 2.29 (s, 3H), 2.33 (s, 6H), 2.47 (s, 11H), 3.78 (m, 2H), 4.13 (s, 4H), 6.99 (s, 2H), 7.10 (s, 2H), 7.33 (d, J = 8.8 Hz, 1H), 7.61 (d, J = 2.2 Hz, 1H), 8.42 (dd, J = 2.6, 8.8 Hz, 1H), 16.71 ppm (s, 1H); ^{13}C NMR (125 MHz, $CDCl_3$): δ = 19.0, 20.6, 21.3, 23.4, 52.0, 59.5, 114.5, 122.3, 123.6, 129.7, 139.5, 148.6, 154.2, 209.2, 295.2 ppm; HRMS (FAB): *m*/*z*: calcd for $C_{32}H_{38}Cl_2N_4O_2Ru$: 682.14 $[M]^+$; found: 682.12.

Compound ***29***: The crude product was purified by chromatography on silica gel (7:3 *n*-hexane/acetone) to give **29** as a dark-green solid (37.4 mg, 40%). Crystals suitable for X-ray analysis were obtained by slow diffusion between hexanes and a solution of **24** in dichloromethane at 4°C. ^{1}H NMR (500 MHz, CD_2Cl_2, 250 K): δ = 1.14 (m, 2H), 1.52 (m, 2H), 2.31 (s, 3H), 2.37 (s, 6H), 2.39 (m, 2H), 2.42 (s, 3H), 2.51 (s, 6H), 3.74 (s, 3H), 3.77 (m, 2H), 4.12 (s, 4H), 6.30 (s, 1H), 6.99 (s, 2H), 7.08 (s, 2H), 7.10 (s, 1H), 7.10 (s, 1H), 16.75 ppm (s, 1H); ^{13}C NMR (125 MHz, CD_2Cl_2): δ = 18.9, 20.8, 21.3, 23.1, 52.1, 56.0, 59.0, 104.4, 114.4, 123.2, 129.6, 139.1, 141.1, 157.1, 160.0, 211.6, 300.9 ppm; HRMS (FAB): *m*/*z*: calcd for $C_{33}H_{41}Cl_2N_3ORu$: 667.17 $[M]^+$; found: 667.27.

Compound ***30***: The crude product was purified by chromatography on silica gel (7:3 *n*-hexane/acetone) to give **30** as a dark-green solid (50.0 mg, 52%). Crystals suitable for X-ray analysis were obtained by slow diffusion between pentane and a solution of **25** in dichloromethane at 4°C. ^{1}H NMR (500 MHz, CD_2Cl_2): δ = 0.83 (d, J = 6.5 Hz, 3H), 1.50 (d, J = 7.3 Hz, 3H), 1.60 (s, 3H), 2.09 (s, 3H), 2.13 (s, 3H), 2.39 (s, 3H), 2.46 (s, 3H), 2.58 (s, 3H), 2.63 (s, 3H), 3.78 (m, 1H), 3.84 (m, 1H), 3.91 (m, 1H), 4.04 (m, 1H), 4.14 (m, 1H), 6.02 (s, 1H), 6.98 (s, 1H), 7.06 (s, 1H), 7.14 (s, 1H), 7.63 (m, 2H), 8.34 (dd, J = 2.2, 8.7 Hz, 1H), 17.18 ppm (s, 1H); ^{13}C NMR (125 MHz, CD_2Cl_2): δ = 18.0, 18.9, 19.9, 20.5, 20.9, 21.3, 21.5, 24.4, 40.5, 51.7, 51.9, 117.3, 122.2, 128.7, 129.1, 130.1, 130.2, 130.7, 131.1, 131.3, 135.8, 137.3, 138.4, 139.8, 140.6, 141.0, 142.7, 149.7, 156.6, 212.4, 280.5 ppm; HRMS (FAB): *m*/*z*: calcd for $C_{31}H_{43}Cl_2N_3O_2RuS$: 693.15 $[M]^+$; found: 693.10.

Compound 31: Compound **25** (0.05 g, 0.21 mmol), CuCl (0.021 g, 0.21 mmol) and anhydrous CH_2Cl_2 (14 mL) were placed in a Schlenk flask. Grubbs second-generation carbene complex (0.161 g, 0.19 mmol) was added and the solution was stirred under argon at 40°C for 30 min. From this point forth all manipulations were carried out in air with reagent-grade solvents. The reaction mixture was concentrated under vacuum and the residue was dissolved in ethyl acetate (5 mL). The white precipitate was filtered off and the filtrate was concentrated under vacuum. The product was purified by column chromatography (*c*-hexane, then 1:1 *c*-hexane/ethyl acetate); compound **31** was separated as a light-green band. The solvent was evaporated under reduced pressure, the product was dissolved in a small amount of ethyl acetate and *n*-heptane was added until green crystals precipitated. The precipitate was filtered off, washed with *n*-heptane and dried in vacuo to afford complex **31** as a light-green solid (0.12 mmol, 0.084 g, 65%). Crystals suitable for X-ray analysis were obtained by slow diffusion between *n*-hexane and a solution of **31** in dichloromethane at 4°C. The additional oxygen atom in the coordination sphere of ruthenium in the crystal structure of complex **31** belongs to a water molecule, which is present in the crystal structure of the complex (Figure 1 f), but we see no evidence for it in the NMR spectra or elemental analysis. ^{1}H NMR (500 MHz, $CDCl_3$): δ = 0.88–0.91 (m, 3H), 1.06–1.68 (m, 6H), 2.30–2.50 (m, 12H), 2.55–2.60 (m, 6H), 3.41 (septet, J = 6.8 Hz, 1H) 4.14 (s, 4H), 7.04–7.06 (m, 2H), 7.08–7.11 (m, 2H), 7.50–7.54 (m, 1H), 7.85–7.87 (m, 1H) 8.50–8.52 (m, 1H), 16.64 ppm (s, 1H); ^{13}C NMR (125 MHz, $CDCl_3$): δ = 15.7, 15.8, 19.1, 21.0, 51.8, 52.7, 114.6, 121.9, 128.0, 129.7, 129.9, 138.1, 138.4, 145.0, 151.8, 156.4, 204.8, 297.3 ppm; IR (KBr): $\tilde{\nu}$ = 3590, 3414, 3082, 2958, 2923, 2867, 1636, 1600, 1525, 1482, 1428, 1380, 1346, 1317, 1267, 1212, 1188, 1109, 1085, 1039, 904, 856, 832, 817, 741, 717, 702, 627, 605, 591, 581, 539, 476 cm^{-1}; HRMS (ESI): *m*/*z*: calcd for $C_{31}H_{37}Cl_2N_2O_3SRu$: 703.70; found: 703.60; elemental analysis calcd (%) for $C_{31}H_{37}Cl_2N_3O_3SRu$: C 52.91, H 5.30, S 4.56, N 5.97; found: C 52.69, H 5.53, S 4.60, N 5.77.

General procedure for metathesis reactions: Olefin (0.2 mmol) and catalyst (0.002 mmol) were dissolved in toluene (2 mL) in a 5 mL round-bottomed flask topped with a reflux condenser under dry nitrogen. The reaction mixture was heated at reflux temperature and monitored by GC–MS.

General procedure for metathesis reactions with catalysts 2 and 3: Olefin (0.350 mmol) and catalyst (0.004 mmol) were dissolved in dichloromethane (17.5 mL) in a 25 mL round-bottomed flask under dry argon. The same conditions were applied for providing metathesis reactions at 0°C, as well as, at 24°C.

Acknowledgements

The Israel Science Foundation and the Edmond J. Safra Foundation are gratefully acknowledged for financial support (N.G.L., A.B., E.T.). K.G. and K.W. thank the Foundation for Polish Science for the "Mistrz" professorships. A.S. and K.G. are grateful for the grant number N N204157636, which was provided by the Polish Ministry of Science and Higher Education. A.S. thanks the Foundation for Polish Science for the START fellowship.

[1] For selected reviews on olefin metathesis, see: a) T. M. Trnka, R. H. Grubbs, *Acc. Chem. Res.* **2001**, *34*, 18–29; b) R. H. Grubbs, *Handbook of Metathesis*, Wiley, Weinheim, **2003**; c) S. J. Connon, S. Blechert, *Angew. Chem.* **2003**, *115*, 1944–1968; *Angew. Chem. Int. Ed.* **2003**, *42*, 1900–1923; d) D. Astruc, *New J. Chem.* **2005**, *29*, 42–56; e) H. Clavier, K. Grela, A. Kirschning, M. Mauduit, S. P. Nolan, *Angew. Chem.* **2007**, *119*, 6906–6922; *Angew. Chem. Int. Ed.* **2007**, *46*, 6786–6801; f) E. Colacino, J. Martinez, F. Lamaty, *Coord. Chem. Rev.* **2007**, *251*, 726–764; g) M. Bieniek, A. Michrowska, D. L. Usanov, K. Grela, *Chem. Eur. J.* **2008**, *14*, 806–818; h) V. Dragutan, I. Dragutan, F. Verpoort, *Platinum Met. Rev.* **2005**, *49*,33–40; i) C. E. Diesendruck, E. Tzur, N. G. Lemcoff, *Eur. J. Inorg. Chem.* **2009**, 4185–4203.

[2] a) P. Schwab, M. B. France, J. W. Ziller, R. H. Grubbs, *Angew. Chem.* **1995**, *107*, 2179–2181; *Angew. Chem. Int. Ed. Engl.* **1995**, *34*, 2039–2041; b) P. Schwab, R. H. Grubbs, J. W. Ziller, *J. Am. Chem. Soc.* **1996**, *118*, 100–110.

[3] a) M. Scholl, S. Ding, C. W. Lee, R. H. Grubbs, *Org. Lett.* **1999**, *1*, 953–956; b) T. M. Trnka, J. P. Morgan, M. S. Sanford, T. E. Wilhelm, M. Scholl, T.-L. Choi, S. Ding, M. W. Day, R. H. Grubbs, *J. Am. Chem. Soc.* **2003**, *125*, 2546–2558.

[4] a) S. B. Garber, J. S. Kingsbury, B. L. Gray, A. H. Hoveyda, *J. Am. Chem. Soc.* **2000**, *122*, 8168–8179; b) S. Gessler, S. Randl, S. Blechert, *Tetrahedron Lett.* **2000**, *41*, 9973–9976.

[5] a) T. Kost, M. Sigalov, I. Goldberg, A. Ben-Asuly, N. G. Lemcoff, *J. Organomet. Chem.* **2008**, *693*, 2200–2203; b) A. Hejl, M. W. Day, R. H. Grubbs, *Organometallics* **2006**, *25*, 6149–6154.

[6] C. Slugovc, D. Burtscher, F. Stelzer, K. Mereiter, *Organometallics* **2005**, *24*, 2255–2258.

[7] a) A. Ben-Asuly, E. Tzur, C. E. Diesendruck, M. Sigalov, I. Goldberg, N. G. Lemcoff, *Organometallics* **2008**, *27*, 811–813; b) X. Gstrein, D. Burtscher, A. Szadkowska, M. Barbasiewicz, F. Stelzer, K. Grela, C. Slugovc, *J. Polym. Sci. Polym. Chem. Ed.* **2007**, *45*, 3494–3500; c) C. E. Diesendruck, Y. Vidavsky, A. Ben-Asuly, N. G. Lemcoff, *J. Polym. Sci. Polym. Chem. Ed.* **2009**, *47*, 4209–4213.

[8] a) K. Grela, S. Harutyunyan, A. Michrowska, *Angew. Chem.* **2002**, *114*, 4210–4212; *Angew. Chem. Int. Ed.* **2002**, *41*, 4038–4040; b) K. Grela, M. Kim, *Eur. J. Org. Chem.* **2003**, 963–966; c) M. Zaja, S. J. Connon, A. M. Dunne, M. Rivard, N. Buschmann, J. Jiricek, S. Ble-

chert, *Tetrahedron* **2003**, *59*, 6545–6558; d) M. Barbasiewicz, M. Bieniek, A. Michrowska, A. Szadkowska, A. Makal, K. Wozniak, K. Grela, *Adv. Synth. Catal.* **2007**, *349*, 193–203; e) R. Ettari, N. Micale, *J. Organomet. Chem.* **2007**, *692*, 3574–3576; f) J. J. Van Veldhuizen, D. G. Gillingham, S. B. Garber, O. Kataoka, A. H. Hoveyda, *J. Am. Chem. Soc.* **2003**, *125*, 12502–12508.

[9] For papers on latent catalysts, see: a) S. Monsaert, A. Lozano Vila, R. Drozdzak, P. Van Der Voort, F. Verpoort, *Chem. Soc. Rev.* **2009**, *38*, 3360–3372; b) S. Monsaert, R. Drozdzak, F. Verpoort, *Chim. Oggi* **2008**, *26*, 93—96; c) F. Ding, Y. Sun, S. Monsaert, R. Drozdzak, I. Dragutan, V. Dragutan, F. Verpoort, *Curr. Org. Synth.* **2008**, *5*, 291–304; d) C. E. Diesendruck, O. Iliashevsky, A. Ben-Asuly, I. Goldberg, N. G. Lemcoff, *Macromol. Symp.* **2010**.

[10] H. Wakamatsu, S. Blechert, *Angew. Chem.* **2002**, *114*, 2509–2511; *Angew. Chem. Int. Ed.* **2002**, *41*, 2403–2405.

[11] A. Szadkowska, A. Makal, K. Wozniak, R. Kadyrov, K. Grela, *Organometallics* **2009**, *28*, 2693–2700.

[12] a) R. Gawin, A. Makal, K. Wozniak, M. Mauduit, K. Grela, *Angew. Chem.* **2007**, *119*, 7344–7347; *Angew. Chem. Int. Ed.* **2007**, *46*, 7206–7209; b) S. L. Balof, B. Yu, A. B. Lowe, Ya. Ling, Y. Zhang, H. J. Schanz, *Eur. J. Inorg. Chem.* **2009**, *13*, 1717–1722; c) S. L. Balof, S. J. P'Pool, N. J. Berger, E. J. Valente, A. M. Shiller, H. J. Schanz, *Dalton Trans.* **2008**, *42*, 5791–5799.

[13] S. J. P'Pool, H. J. Schanz, *J. Am. Chem. Soc.* **2007**, *129*, 14200–14212.

[14] A. Ben-Asuly, A. Aharoni, C. E. Diesendruck, Y. Vidavsky, I. Goldberg, B. F. Straub, N. G. Lemcoff, *Organometallics* **2009**, *28*, 4652–4655.

[15] F. H. Allen, *Acta Crystallogr. Sect. B* **2002**, *58*, 380–388.

[16] T. Ritter, A. Hejl, A. G. Wenzel, T. W. Funk, R. H. Grubbs, *Organometallics* **2006**, *25*, 5740–5745.

[17] a) C. E. Diesendruck, E. Tzur, A. Ben-Asuly, I. Goldberg, B. F. Straub, N. G. Lemcoff, *Inorg. Chem.* **2009**, *48*, 10819–10825; b) M. Barbasiewicz, A. Szadkowska, R. Bujok, K. Grela, *Organometallics* **2006**, *25*, 3599–3604; c) C. Slugovc, B. Perner, F. Stelzer, K. Mereiter, *Organometallics* **2004**, *23*, 3622–3626; d) T. Ung, A. Hejl, R. H. Grubbs, Y. Schrodi, *Organometallics* **2004**, *23*, 5399–5401.

[18] For an alternative synthesis, see: J. Mihailo, *Z. Anorg. Allg. Chem.* **1956**, *288*, 324–328.

[19] J. Kruszewski, T. M. Krygowski, *Tetrahedron Lett.* **1972**, *13*, 3842–3842.

Received: December 17, 2009
Published online: June 16, 2010

